Oral presentation | 4 JSAP-Optica Joint Symposia 2024：4.7 Quantum Optics, Nonlinear Optics and Structured Optics

Fri. Sep 20, 2024 10:00 AM - 11:30 AM JST | Fri. Sep 20, 2024 1:00 AM - 2:30 AM UTC C43 (Hotel Nikko 4F)

[20a-C43-1~5] 4.7 Quantum Optics, Nonlinear Optics and Structured Optics

Sunao Kurimura(NIMS)

English Presentation
10:00 AM - 10:30 AM JST | 1:00 AM - 1:30 AM UTC
[20a-C43-1]
[JSAP-Optica Joint Symposia Invited Talk] Femtosecond Region Photon Echo with Quantum Dots via Up-conversion Single-photon Detector

○Yuta Kochi[1,2], Sunao Kurimura[3], Kouichi Akahane[4], Junko Ishi-Hayase[1,2] (1.Keio Univ., 2.Keio CSRN, 3.NIMS, 4.NICT)

English Presentation
10:30 AM - 10:45 AM JST | 1:30 AM - 1:45 AM UTC
[20a-C43-2]
Optimizing Spontaneous Parametric Down Conversion in Metasurfaces with In-verse Design

○Marcus Cai[1], Neuton Li[1], Tongmiao Fan[1], Jihua Zhang[1,2], Jinyong Ma[1], Dragomir Neshev[1], Andrey Sukhorukov[1] (1.ARC Centre of Excellence for Transformative Meta-Optical Systems (TMOS), Dept. of Electronic Materials Engineering, Research School of Physics, Australian National Univ., Australia, 2.Songshan Lake Materials Lab., China)

Presentation by Applicant for JSAP Young Scientists Presentation Award English Presentation
10:45 AM - 11:00 AM JST | 1:45 AM - 2:00 AM UTC
[20a-C43-3]
Spectral resolution of quantum Fourier transform infrared spectroscopy using pulsed laser excitation

○(DC)Jasleen Kaur[1], Yu Mukai[1], Ryo Okamoto[1], Shigeki Takeuchi[1] (1.Kyoto University)

English Presentation
11:00 AM - 11:15 AM JST | 2:00 AM - 2:15 AM UTC
[20a-C43-4]
All-fiber broadband photon pair generation in dispersion flattened highly non-linear fiber

○(D)Anadi Agnihotri[1], Pradeep kumar Krishnamurthy[1] (1.IIT Kanpur)

English Presentation
11:15 AM - 11:30 AM JST | 2:15 AM - 2:30 AM UTC
[20a-C43-5]
Quantum Antibunching in Nonlinear Coupler Using Wigner Representation

Mohd Syafiq M. Hanapi[1], Abel-Baset M. A. Ibrahim[1], ○Pankaj Kumar Choudhury[2] (1.Univ. Teknologi MARA, 2.Zhejiang University)

Femtosecond Regime Photon Echo with Quantum Dots Evaluated by Up-conversion Single-photon Detector

Yuta Kochi[1, 2], Sunao Kurimura[3], Kouichi Akahane[4] and Junko Ishi-Hayase[1, 2]
[1] School of Fundamental Science and Technology, Keio University
[2] Center for Spintronics Research Network, Keio University
[3] National Institute for Materials Science
[4] National Institute of Information and Communications Technology
E-mail : yuta.kouchi@keio.jp

Introduction

Recently, quantum information processing and communications using photons have been attracting attention. To increase the density of transmitted photonic qubits, it is necessary to develop broadband quantum memories and detectors that can handle ultrashort pulses. Although rare-earth-ion doped quantum memories [1] have been widely studied, due to their storage bandwidth of ~GHz, they are incapable of storing ultrashort pulses. In our group, we used the photon echo (PE) method with quantum dots (QDs) to realize ultrashort femtosecond pulse storage. However, we encountered many difficulties in realizing this method such as low PE efficiency from the QDs and the insufficient temporal resolution of the avalanche single-photon detectors. To solve these problems, we have applied a new quantum control method and utilized an up-conversion single-photon detector (UCSPD) [2]. In this presentation, we will introduce the techniques "1. Time-resolving measurement by UCSPD," "2. PE quantum memory using QDs" and "3. enhancement of PE signals."

1. Time-resolving measurement by UCSPD

To enable femtosecond regime time-resolving measurements, we developed a UCSPD. This single-photon detector uses the frequency up-conversion technique and signal photons are converted to visible photons by sum-frequency generation (SFG). For this process, we used a femtosecond pulse laser as the pump light. Since SFG occurs only when the signal photons and the pump pulse overlap, we can perform time-gating the signal waveforms with femtosecond order temporal resolution. Fig. 1(a) shows the schematic setup of the UCSPD. The up-conversion efficiency in the femtosecond regime strongly depends on crystal length because of the group delay between signal and pump pulses in a crystal. Despite much research on up-conversion with CW laser, SFG between femtosecond pulses has rarely been investigated. Hence, we evaluated the crystal length dependence of UCSPD performances theoretically and experimentally and achieved the temporal resolution of 415 fs. Our results provide a guideline for optimizing crystal length for femtosecond up-conversion.

2. PE quantum memory using QDs

As a demonstration of our UCSPD, we detected femtosecond PE from InAs QDs with an inhomogeneous broadening of 7.2 THs. By applying the PE method, we can use these QDs as a medium for broadband quantum memory. We successfully stored 200 fs time-bin pulse in our QDs, read-out the stored signals, and measured the waveforms by UCSPD for the first time (Fig. 1(b)). We also succeeded in evaluating the relative phase of time-bin PE signals with a visibility of over 90 %.

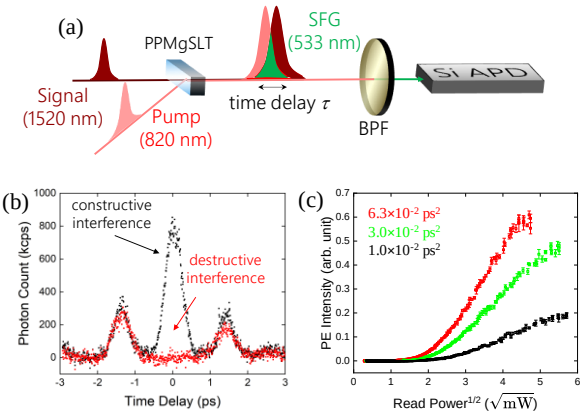

Fig. 1 (a) Optical setup of UCSPD. (b) Temporal waveforms of time-bin PE with different phase. (c) Chirped amount dependence of PE signal intensity.

3. Enhancement of PE signal using chirped pulses

Since we applied a rephasing pulse to read-out stored signals as an echo signal for the PE method, the accuracy of quantum control directly affects memory efficiency. Extending the bandwidth of QDs to THz is complicated because large detuning makes it difficult to accurately control the system through single-frequency pulses. To solve this problem, we introduced the adiabatic rapid passage (ARP) method [3], which uses chirped pulses for read-out and enables robust control. Although this method has been demonstrated only for rare-earth-ion-doped materials, we have demonstrated that ARP is also effective for QDs with inhomogeneous broadening more than 100 times wider than in conventional methods. Fig. 1(c) shows the chirped amount dependence of PE intensity. These results are a great achievement for advancing into the femtosecond regime of quantum communications.

This work was partly supported by CSRN, Keio University. The QDs sample was fabricated at Advanced ICT Laboratory, NICT. The authors would like to thank Prof. R. Shimizu, Y. Kinoshita, M. Hornauer, Y. Takahashi, and T. Shoji for their useful discussion.

References

[1] Z. Q. Zhou, *et al.*, Laser Photonics Rev., **17**, 2300257 (2023).
[2] Y. Kochi, *et al.*, arXiv, 2205.06957 (2022).
[3] G. Demeter, *et al.*, Phys. Rev. **A**, **88**, 052316 (2013).

Optimizing Spontaneous Parametric Down Conversion in Metasurfaces with Inverse Design

Marcus Cai[1], Neuton Li[1], Tongmiao Fan[1], Jihua Zhang[1,2], Jinyong Ma[1], Dragomir N. Neshev[1], Andrey A. Sukhorukov[1]

[1] ARC Centre of Excellence for Transformative Meta-Optical Systems (TMOS), Department of Electronic Materials Engineering, Research School of Physics, Australian National University, Canberra, Australia
[2] Songshan Lake Materials Laboratory, Dongguan, Guangdong, P.R. China
E-mail: marcus.cai@anu.edu.au

Spontaneous parametric down conversion (SPDC) is one of the most versatile techniques for the generation of correlated photon pair, whose quantum state is essential for photon entanglement that underpins many quantum applications like secure communication, quantum metrology and lithography and quantum imaging [1]. Inverse design of effective SPDC has been achieved by structured crystals with shaped pump beams [2]. Another popular platform for SPDC is nanofabricated structures with sub-wavelength thickness called metasurfaces, as they could achieve drastic enhancement of nonlinear light-matter interactions [3]. There remains the possibility to use inverse design to optimize metasurfaces for SPDC.

In this work, we report a method for optimizing metasurfaces' SPDC performance by building on an existing inverse design optimization framework [4]. Our method employs a gradient-based optimization method called adjoint optimization and the quantum-classical correspondence between SPDC and Sum Frequency Generation [5]. By strategically setting our desired output function in the algorithm, we can control the degree of polarization entanglement we optimize for. We create patterns for unidirectional SPDC that outperform the thin film of the same material and thickness by more than 10 times in brightness while ensuring the almost maximal polarization entanglement of the signal and idler states.

Our results show the possibility of inversely designing metasurfaces with good SPDC that produce strongly entangled signal and idler states, allowing various quantum applications like secure communication and quantum metrology. By building on our work, we can further explore the direction of the signal, idler and pump photons.

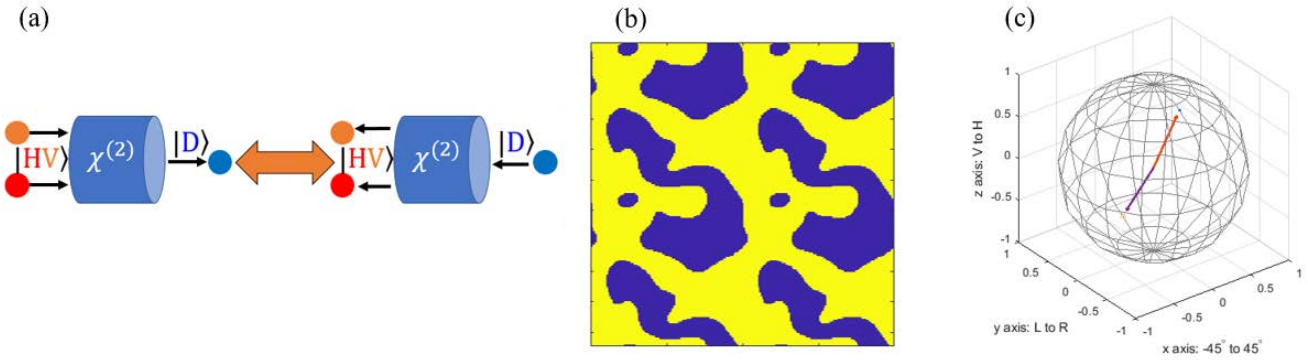

Fig. 1. (a) Diagram of the quantum-classical correspondence of SPDC and SFG: Signal (idler) photon is horizontally (vertically) polarized while the pump photon is diagonally polarized. The second-order nonlinear material is InGaP in our case. (b) Optimized pattern that provides good SPDC performance while trying to maximize the entanglement of the signal and idler states. (c) Poincare-sphere representation of the signal and idler states from SPDC: Each axis represents the corresponding polarization from negative 1 to positive 1. For example, y=-1 represents left-handed circular polarization while y=1 right-handed circular polarization [6]. Vectors pointing in opposite directions means maximal entanglement.

References

[1] J. L. O'Brien, A. Furusawa, and J. Vučković, Nature Photon. 3, 687–695 (2009).
[2] E. Rozenberg, A. Karnieli, O. Yesharim, J. Foley-Comer, S. Trajtenberg-Mills, D. Freedman, A. M. Bronstein, and A. Arie, Optica 9, 602-615 (2022).
[3] A. H. Dorrah and F. Capasso, Science 376, 367 (2022).
[4] N. Li, J. Zhang, D. N. Neshev, and A. A. Sukhorukov, Nanophotonics, 137 (2024).
[5] A. N. Poddubny, I. V. Iorsh, and A. A. Sukhorukov, Phys. Rev. Lett. 117, 123901 (2016).
[6] M. V. Chekhova and M. V. Fedorov, J. Phys. B 46, 095502 (2013).

Spectral resolution of quantum Fourier transform infrared spectroscopy using pulsed laser excitation

Jasleen Kaur, Yu Mukai, Ryo Okamoto, Shigeki Takeuchi*
Kyoto University
*E-mail: takeuchi@kuee.kyoto-u.ac.jp

1. Introduction

In recent years, nonlinear quantum interferometry has been widely explored for applications like spectroscopy, optical coherence tomography, and imaging [1]. Quantum infrared spectroscopy (QIRS) uses quantum interference of generation processes of frequency-entangled visible-IR photon pairs to perform infrared spectroscopy using visible light sources and silicon-based detectors [2]. This technique utilizes a nonlinear quantum interferometer configuration where the generated IR photons pass through the sample, and the correlated visible photons are detected. The change in the detected visible photon flux with and without the sample helps extract the complex transmittance of the sample in the IR region.

It is commonly assumed that perfect frequency correlation between visible and IR photons is essential for achieving high spectral resolution in QIRS. Therefore, continuous wave (cw) lasers with negligible linewidth are predominantly used in most QIRS experiments. Conversely, when using pulsed lasers, the inherent finite spectral linewidth is generally thought to degrade the spectral resolution. Recently, we reported that the visibility of spectral-domain quantum interference decreases for pulsed pumping [3], confirming that spectral resolution of dispersive QIRS method degrades, wherein a dispersive spectrometer is used for detection. However, pulsed pumping is attractive as it enables high generation efficiency of visible-IR photons and time-resolved measurements.

Here, we investigate whether high spectral resolution can be obtained with a pulsed pump of finite spectral linewidth using the quantum Fourier-transform infrared (QFTIR) spectroscopy method. In this method, interferogram of visible photons is recorded while scanning the optical path difference between nonlinear interferometer arms. Taking the ratio of Fourier amplitudes of interferograms with and without sample, we can extract the spectrum of sample in IR region [4]. In this presentation, we will report the theoretical framework of QFTIR with pulsed pumping. We also plan to experimentally show whether high-resolution spectra of samples can be observed with pulsed pumping.

2. Experimental setup

Figure 1 shows the experimental setup consisting of both pulsed and cw lasers to allow a fair comparison under the same experimental conditions. The cw pump has center wavelength of 532.37 nm, average power of 150 mW, and negligible linewidth (<1 MHz). The pulsed laser source of 532 nm centroid wavelength has linewidth of ~0.6 nm

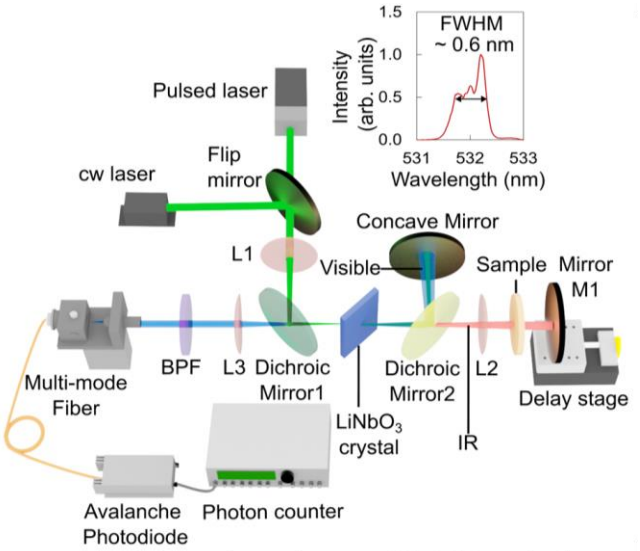

Fig. 1: Experimental setup of QFTIR method

(pulsed laser spectrum in inset of Fig. 1) and an average power of 150 mW. The visible photon interferograms are recorded for both pump sources. The pump beam passes through 0.5 mm thick MgO:$LiNbO_3$ crystal, generating visible-IR photon pairs of about 816 nm and 1.53 µm. Quantum interference occurs between generation processes and visible photon interferogram is detected by Si photodiode while scanning mirror M1 placed on delay stage.

3. Conclusion

We will present a theoretical and experimental investigation of the effect of pulsed laser linewidth on the spectral resolution of the QFTIR method. Our results will be useful for performing high-resolution ultrafast infrared spectroscopy using a visible light source and detector.

Acknowledgments

This work is supported by MEXT Quantum Leap Flagship Program Grant Number JPMXS0118067634; Cabinet Office, Government of Japan, Public/Private R&D Investment Strategic Expansion Program (PRISM); JSPS KAKENHI Grant Number 21H04444; and WISE Program, MEXT.

References

[1] A. Hochrainer, M. Lahiri, M. Erhard, M. Krenn, and A. Zeilinger, Rev. Mod. Phys. 94, 025007 (2022).
[2] D. A. Kalashnikov, A. V. Paterova, S. P. Kulik, and L. A. Krivitsky, Nature Photonics 10, 98 (2016).
[3] J. Kaur, Y. Mukai, R. Okamoto, and S. Takeuchi, Phys. Rev.A 108, 063714 (2023).
[4] Y. Mukai, M. Arahata, T. Tashima, R. Okamoto, and S. Takeuchi, Phys. Rev. Applied 15, 034019 (2021).

All-fiber broadband photon pair generation in dispersion flattened highly non-linear fiber

Indian Institute of Technology Kanpur.[1], **°Anadi Agnihotri**[1], **Pradeep Kumar Krishnamurthy**[1]

E-mail: anadi@iitk.ac.in

We report on a spontaneous four-wave mixing (SFWM) based broadband correlated photon pair generation using a dispersion flattened highly-nonlinear fiber (DF-HNLF). The DF-HNLF is pumped by a stable mode-locked laser (MLL) which generates pump pulses of 250 ps FWHM at a repetition rate of 94.509 MHz. The joint spectral intensity (JSI) data indicates photon pair generation across entire S, C, and L bands. The intrinsic photon pair generation rate, after accounting for spontaneous Raman scattering (SpRS), system loss, and detector dark counts, is ≈ 100kHz although due to detection gating limit we measured the rate to be 1 kHz at peak pump power of 70 mW. The use of an arbitrary waveform generator for establishing pump MLL and gating of the single-photon detectors (SPDs) allows for precise synchronization of generation and detection of photon pairs.

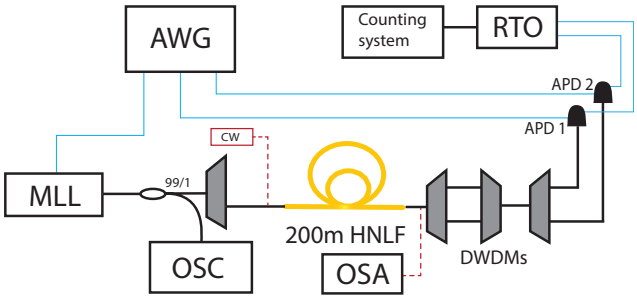

Figure 1: Schematic diagram of experimental setup for broadband photon pair generation.

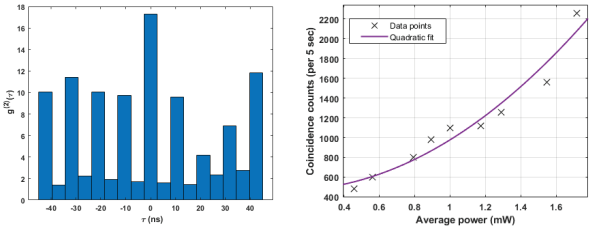

(a) (b)

Figure 2: Photon pair measurement results for signal at 1552.52 nm and idler at 1547.72 nm (a) Cross-correlation measurement for 1 mW of average pump power, (b) Coincidence counts vs pump power.

Fig. 1. shows the schematic diagram of our experimental setup. The pulses from the MLL is coupled into a 200 m DF-HNLF from OFS. For the JSI measurement as in [1], a CW laser output from a tunable laser diode is coupled along with the pump as shown in dashed lines. At the output of the HNLF, the signal and idler wavelengths are filtered out and

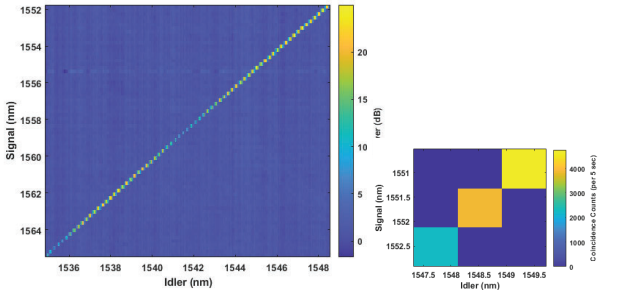

(a) C-band (b) C- band coincidenc counts

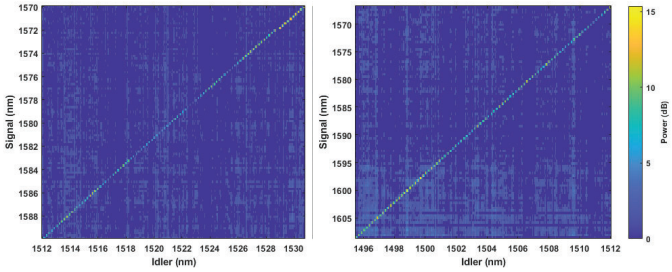

(c) S and L band (d) S and L band

Figure 3: Measured Joint Spectral Intensiy of photon pairs generated in dispersion flattened 200m HNLF

pump is suppressed using a set of DWDM filters with FWHM bandwidth of 0.8 nm. The signal and idler are detected using a pair of SPDs gated at ninetieth of MLL repetition rate, i.e., 1.05 MHz. This is due to the circuit limitation of the SPD and not due to the setup itself. An AWG provides gating pulses to both SPDs with a tunable delay so as to measure the photon statistics. Fig. 2(a) shows the coincidence count measurements between signal and idler. The histograms are plotted by collecting 5×10^6 samples for each delay. The 0 ns delay counts are mainly due to the SFWM interaction while the peaks at other delays, taken at pulse repetition rate, are due to SpRS and detector dark counts. Fig. 2(b) plots the coincidence counts at signal and idlers at 1552.52 and 1547.72 nm as a function of average pump power. We see that the coincidence count is a quadratic function indicating that the setup emits entangled photon pairs in this operational regime [2]. Fig. 3 shows JSI across 1500-1600 nm covering S,C, and L bands. The coincidence counts at ITU grid wavelengths in C-band are shown in Fig. 3(b).

References

1. B. Fang, O. Cohen, M. Liscidini, *et al.*, Optica **1**, 281 (2014).
2. X. Li, J. Chen, P. Voss, *et al.*, Opt. Express **12**, 3737 (2004).

Quantum Antibunching in Nonlinear Coupler Using Wigner Representation

Mohd Syafiq M. Hanapi[1], Abel-Baset M. A. Ibrahim[1], Pankaj K. Choudhury[2*]

[1]Faculty of Applied Sciences, Universiti Teknologi MARA, 40450 Shah Alam, Selangor, Malaysia
[2]International Research Center for Advanced Photonics, Zhejiang University, Building 1A, 718 East Haizhou Rd., Haining, Zhejiang 314400, P. R. China
[*]E-mail : pkchoudhury@ieee.org

1. Introduction

Antibunching, a key characteristic of single-photon sources, is crucial for quantum cryptography and quantum computing [1]. Nonlinear couplers have significant potential as generators of nonclassical light [2,3]. However, Limited research has been reported on antibunching in nonlinear couplers [4,5]. This study investigates antibunching in an innovative design of a nonlinear coupler (as fig. 1 shows) featuring three nonlinear waveguides, each comprising a material that exhibits the second-order nonlinearity.

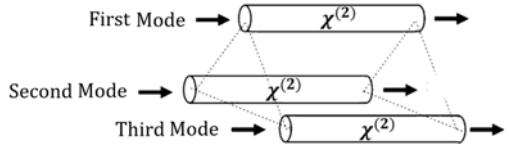

Fig. 1. Schematic of three-channel nonlinear coupler operating with SHG.

2. The model

With reference to fig. 1, we assume the interaction of light with the nonlinear waveguide material produces second-harmonic generation (SHG). The Hamiltonian for this three-mode system can be expressed in the form as [6]

$$\frac{\hat{H}}{\hbar} = \sum_j^3 \omega_j \hat{a}_j^\dagger \hat{a}_j + 2\sum_j^3 \omega_j \hat{b}_j^\dagger \hat{b}_j + \frac{ig}{2}\sum_j^3 \left(\hat{a}_j^2 \hat{b}_j^\dagger - \text{h.c.}\right) + \kappa\left(\hat{a}_1^\dagger \hat{a}_2 + \hat{a}_2^\dagger \hat{a}_3 + \hat{a}_3^\dagger \hat{a}_1 + \text{h.c.}\right). \quad (1)$$

In the Hamiltonian equation, $\hat{a}_j^\dagger \hat{a}_j$ is the ladder operator where j = 1, 2, and 3 that correspond to the first, second, and third modes, respectively. $\hbar$ is the reduced Planck constant, ω_j is the input frequency, g is the nonlinear coupling constant, and κ is the linear coupling parameter. Using this Hamiltonian in symmetrical order, the evolution of the current three-mode system is described using the von Neumann equation to obtain a quantum density master equation. The quantum density matrix equation is then converted to its corresponding classical Fokker-Planck (FP) equation using the Wigner representation. The FP equation is subsequently mapped to a system of stochastic differential equations following Ito calculus. This system is solved numerically, and the antibunching is evaluated using the correlation criteria

$$D_j = \left\langle \left(\Delta \hat{N}_j\right)^2 \right\rangle - \left\langle \hat{N}_j \right\rangle^2. \quad (2)$$

Herein, $\hat{N}_j = \hat{a}_j^\dagger \hat{a}_j$ is a number operator, $\langle \hat{N}_j \rangle$ signifies the average particle or photon count in the j^{th} mode, and the antibunching is indicated by $D_j < 0$.

3. Discussion

Figure 2 illustrates the antibunching behavior in the first channel waveguide for various values of the linear coupling parameter $\tilde{\kappa}$. At $\tilde{\kappa}$ = 0.1 (fig. 2a), the antibunching oscillations are slow. As $\tilde{\kappa}$ increases to 0.3 (fig. 2b) and 0.7 (fig. 2c), the oscillations become more rapid. This behavior is very likely due to narrower channel separation, which allows for more efficient energy exchange between the waveguides (in three-channel nonlinear coupler system), leading to a faster antibunching response.

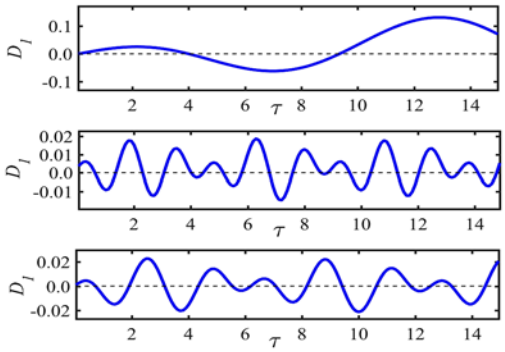

Fig. 2. Photon antibunching exhibited by the first mode. Evolution below the y = 0 line indicates antibunching. (a) $\tilde{\kappa}$ = 0.1, (b) $\tilde{\kappa}$ = 0.3, and (c) $\tilde{\kappa}$ = 0.7. The other input parameters are $\alpha_1 = \alpha_2 = \alpha_3 = 1$, $\tilde{\omega}_1 = \tilde{\omega}_2 = \tilde{\omega}_3 = 1$ and $\tilde{g}$ = 0.01. The dimensionless parameters are related to their dimensionless counterparts by $\tilde{\omega}_1 = \omega_1/\omega_1$, $\tilde{\omega}_2 = \omega_2/\omega_1$, $\tilde{\omega}_3 = \omega_3/\omega_1$, $\tilde{g} = g/\omega_1$, $\tilde{\kappa} = \kappa/\omega_1$, and $\tau = \omega_1 t$.

4. Conclusion

We have investigated the potential for generating photon antibunching in a three-channel waveguide nonlinear coupler system that operates with second-order nonlinearity and produces SHG, using the Wigner representation in phase space. The results demonstrate the effectiveness of a three-channel SHG-based nonlinear coupler in generating quantum antibunching. This simple-structured device would serve as an efficient source of antibunching light.

Acknowledgement

A-BMAI acknowledges the Ministry of Higher Education (MOHE, Malaysia) for the grant FRGS/1/2021/STG07/UITM/02/10 and PKC acknowledges the financial support by Zhejiang University (China) through the grant 1113000*194232301/002.

References

[1] H. Zhu, X. Li, Z. Li, F. Wang, and X. Zhong, Opt. Express **31** (2023) 22030.
[2] M. S. M. Hanapi, A.-B. M. A. Ibrahim, and P. K. Choudhury, Optik **243** (2021) 167420.
[3] R. Julius, A.-B. M. Ibrahim, P. K. Choudhury, A. N. Alias, and M. S. Abd Halim, Sci. Rep. **12** (2022) 8245.
[4] R. Julius, A.-B. M. A. Ibrahim, P. K. Choudhury, and H. Eleuch, Chin Phys B **27** (2018) 114206.
[5] S. Mandal and J. Perina, Phys. Lett. A **328** (2004) 144.
[6] R. Julius, A.-B. M. A. Ibrahim, H. Eleuch, and P. K. Choudhury, J. Mod. Opt. **66** (2019) 1129.